

# Characterization of a Freezing/Melting Transition in a Vibrated and Sheared Granular Medium

Karen E. Daniels<sup>1,2</sup> & Robert P. Behringer<sup>1</sup>

<sup>1</sup>Department of Physics and Center for Nonlinear and Complex Systems, Duke University, Durham, NC, 27708, USA

<sup>2</sup>Department of Physics, North Carolina State University, Raleigh, NC, 27695, USA

E-mail: karen.daniels@ncsu.edu and bob@phy.duke.edu

**Abstract.** We describe experiments on monodisperse spherical particles in an annular cell geometry, vibrated from below and sheared from above. This system shows a freezing/melting transition such that under sufficient vibration a crystallized state is observed, which can be melted by sufficient shear. We characterize the hysteretic transition between these two states, and observe features reminiscent of both a jamming transition and critical phenomena.

PACS numbers: 05.70.Ln, 45.70.-n, 47.57.Gc, 81.05.Rm, 83.80.Fg

Submitted to: Journal of Statistical Mechanics

## 1. Introduction

Granular materials exhibit phases analogous to conventional solids, liquids, and gases, in spite of being athermal and dissipative [1]. Due to the dissipation, energy must be supplied in order to sustain a dynamical state. Shearing and vibration are two common means to inject energy into granular systems. Shearing a granular material can compact and crystallize it [2], but also melt it [3]; tapping will compact it [4]; in thin vibrated layers there can be coexistence of crystallized and disordered states [5]; and highly vibrated granular systems become gas-like. From a large phase space of variables we vary only two, the shear rate and vibration amplitude, and study the interaction of the two energy injection mechanisms.

Without vibration, sheared granular materials undergo a phase transition from solid-like to fluid-like behavior: the particles must become unjammed (which typically involves dilation) before they can move. We seek to understand what effects vibrations have on such transitions, and on the characteristics of the states on either side of the transition. This is particularly interesting given that granular systems are athermal, and one might naively expect that vibrations would play a temperature-like role.

We perform experiments in a classic geometry, annular shear flow [6, 7, 8, 9], with monodisperse particles, shown schematically in Figure 1. Shear and vibration provide competing effects, with the system evolving to a crystallized state when the kinetic energy provided by the vibration is greater than that provided by the shear. The transition is hysteretic, and fluctuations in the packing fraction and the breadth of the force distribution both become large as the crystallized state is approached, in similarity to phase transitions in other systems.

The physical parameters that characterize the system include the amplitude  $A$  and frequency  $f$  of vibration, the height  $H$  and mean radius  $r$  of the annular container, the diameter  $d$  and the density of the particles, the rotation rate of the upper shearing surface, and the mean pressure  $P$  on the layer (here characterized at the base of the layer). From these physical parameters, it is possible to define other dimensioned

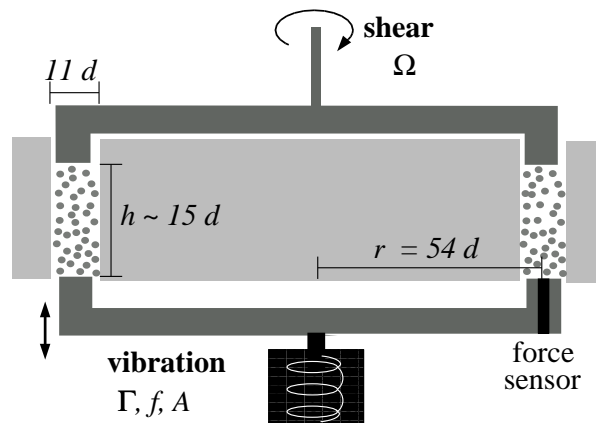


Figure 1. Schematic cross-section of experiment (not to scale).

	$\frac{A \omega^2}{g}$	vibrational acceleration / gravitational acceleration
H	$\frac{h}{d}$	cell height / particle size
I	$\frac{v_d}{c}$	particle scale velocity / acoustic velocity
J	$\frac{v_r}{A \omega}$	apparatus scale velocity / vibration velocity
K	$\frac{A \omega}{c}$	vibration velocity / acoustic velocity
L	$\frac{A}{d}$	vibration length scale / particle length scale
M	$\frac{\dot{\gamma}}{\omega}$	shear time scale / vibration time scale
N	$\frac{P}{g d}$	applied pressure / hydrostatic pressure
R	$\frac{r}{d}$	cell radius / particle diameter
$\sim$	$\frac{v_r}{v_d}$	shear velocity / particle velocity

Table 1. Dimensionless ratios, with  $\omega = 2\pi f$ ,  $\dot{\gamma} = r\dot{\theta}/h$ , and  $c = \sqrt{P/\rho}$ .

parameters, such as the shear rate,  $\dot{\gamma} = r\dot{\theta}/h$ , as well as a number of dimensionless parameters which we list in Table 1.

$\dot{\gamma}$ , I and J are three key parameters from the list in Table 1. Of the ten listed, there are only seven independent parameters: for example,  $\dot{\gamma} = K^2 N/L$  and the four velocity ratios (H; I; J; K) only represent three parameters. In the experiments described here, we have fixed  $f$ ,  $P$ , and  $N$  and therefore only explored a small region of the available phase space.

## 2. Experiment

The experimental apparatus consists of an annular region containing nearly monodisperse polypropylene spheres of diameter  $d = 2.29$  to  $2.39$  mm and density  $\rho = 0.90$  g/cm<sup>3</sup>, as shown in Figure 1, with the pressure  $P$  and volume  $V$  (height  $h$ ) set from below by a spring within an electromagnetic shaker. The particles are sheared from above and vibrated from below, while the sidewalls are stationary. A more detailed description of the apparatus is given in [3]. To characterize the states, we obtain high-speed video images of particles at the outer Plexiglas wall, laser position measurements of the bottom plate (cell volume), and force time series from a capacitive sensor flush with the bottom plate. For the experiments described in this paper, we fix the frequency of vibration ( $f = 60$  Hz) and number of particles ( $N = 71200$ ), and vary the amplitude of vibration  $A$  and shear rate  $\dot{\gamma}$ . We vary the nondimensionalized peak acceleration

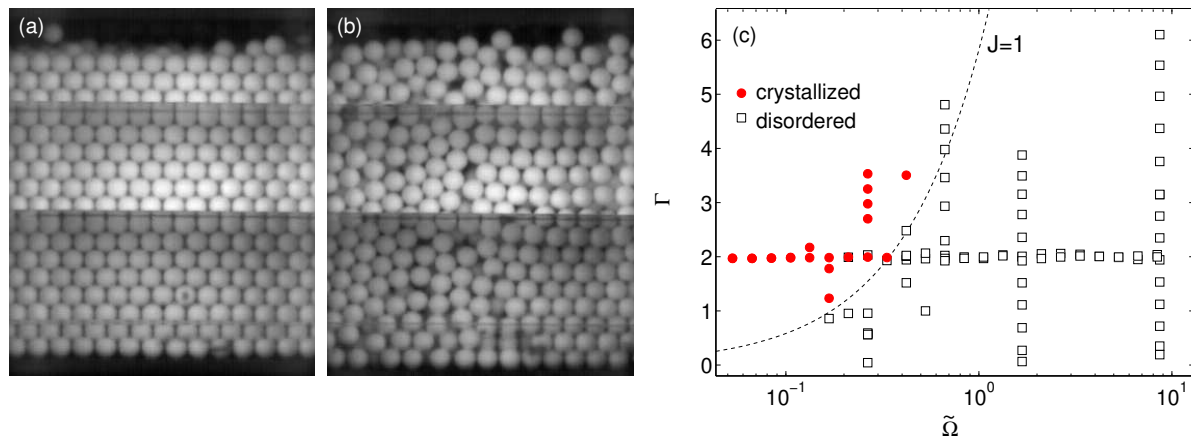


Figure 2. Sample images, viewed from outer wall. (a) Crystallized state:  $\tilde{\Omega} = 2.0$  and  $\tilde{\gamma} = 0.078$ . Movie at <http://nile.physics.ncsu.edu/pub/cryst.mpg> (b) Disordered state:  $\tilde{\Omega} = 2.0$  and  $\tilde{\gamma} = 0.47$ . Linear (L) and hexagonal (H) clusters marked by black boxes. Movie at <http://nile.physics.ncsu.edu/pub/disord.mpg> (c) Phase diagram for crystallized and disordered states as a function of  $\tilde{\Omega}$  and  $\tilde{\gamma}$ . Dashed line is  $J = 1$ . Adapted from [3].

A  $2 \leq \tilde{\gamma} \leq 6$ , and nondimensional shear rate  $\tilde{\Omega} = \frac{p}{\rho g d}$  from 0.058 to 9.3.

### 3. Description of States

In the regime  $0 < \tilde{\Omega} < 10$  and  $0 < \tilde{\gamma} < 6$  we observe two distinct granular states of matter: crystallized and disordered. Sample images and movies of these two states are shown in Figure 2ab, as viewed from the outer wall. For  $\tilde{\Omega} \lesssim 1$  and  $\tilde{\gamma} < 4$ , we observe that the phase boundary between the two states roughly corresponds to a curve where the characteristic velocities of the two motions are equal. This corresponds to the dimensionless number  $J$  of Table 1:

$$J = \frac{r}{2 \tilde{\gamma} A} \quad (1)$$

and the curve  $J = 1$  is shown by the dashed line in Figure 2c. Below, we characterize these two states, with further details to be found in [3].

**Crystallized State:** In the solid-like state (see Figure 2a), the balls crystallize into a hexagonally close-packed configuration (i.e. a 3D crystalline structure) here visible only at the outer wall although the order persists across the layer. The contact between the upper layer of the granular material and the shearing wheel is intermittent, with stick-slip motion of the top 2 layers in the manner of [10]. The distribution of forces measured at the bottom of the layer is bimodal (see Figure 3); this indicates that the material is responding as a solid body moving up and down with the sinusoidal vibrations of the bottom plate.

**Disordered State:** In the disordered state, some order remains in the form of hexagonally-packed clusters and linear chains of particles at the outer wall, as marked

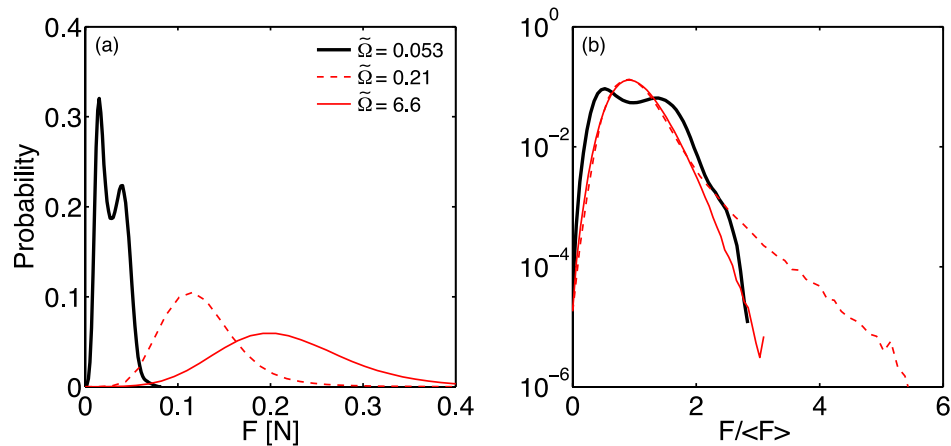


Figure 3. Force probability distribution functions for three values of  $\tilde{\Omega}$  at  $\phi = 2:0$ . (a) on linear scales, dimensioned and (b) on log-linear scales, normalized by mean force.

in Figure 2b. For states with  $\tilde{\Omega}$  well above the transition, linear chains dominate over hexagonal clusters, with both existing intermittently throughout the disordered regime. These chains may correspond to the planar ordering reported recently by Tsai et al. [2, 11]. The velocity profile extends deeper into the layer (in the vertical direction) than in the crystallized state. Force distributions measured at the bottom plate show the exponential-like tails characteristic of many granular experiments in disordered, unvibrated granular materials (see Figure 3). They also fall to zero at low force, as seen in earlier experiments by Miller et al. [7].

For a geometrically similar system, but unvibrated and exposed to a compressional force, shear ordered the system into horizontal planes of hexagonal packing, each slipping past the others [2, 11]. Such a state is different from the 3D crystallized state observed here, in which the layers in the bulk are stationary with respect to each other. An interesting question is how shearing creates order or disorder depending on the presence or absence of vibration. A useful way to distinguish the ordered and disordered regimes is via the ratio

$$I = \frac{\tau_d}{\tau_p} \quad (2)$$

involving the shear time scale  $\tau_d = \eta/h$  to the acoustic time scale,  $\tau_p = \sqrt{\rho/P}$ , calculated from the pressure  $P$  and density  $\rho$  [12]. The experiments described in this paper have pressures of around  $P = 20$  Pa and shear rates of  $\dot{\gamma} = 0.3$  to  $40$  Hz, leading to  $I = 5 \cdot 10^{-3}$  to  $0.75$ . In [2], the shear rates are slower,  $\dot{\gamma} = 0.05$  to  $0.5$  Hz, and pressures are higher,  $P = 2000$  Pa, so that the system is clearly in the quasistatic regime with  $I = 3 \cdot 10^{-5}$  to  $3 \cdot 10^{-4}$ .

While it is perhaps surprising that we find as simple a result as a phase transition at  $J = 1$ , the presence of these other important control parameters give hints into the breakdown of crystallization for large  $\tilde{\Omega}$ . Figure 2c shows that for  $\tilde{\Omega} = 0.7$ , crystallization was not observed above  $\phi = 4$ , possibly indicating the re-emergence of disorder due to

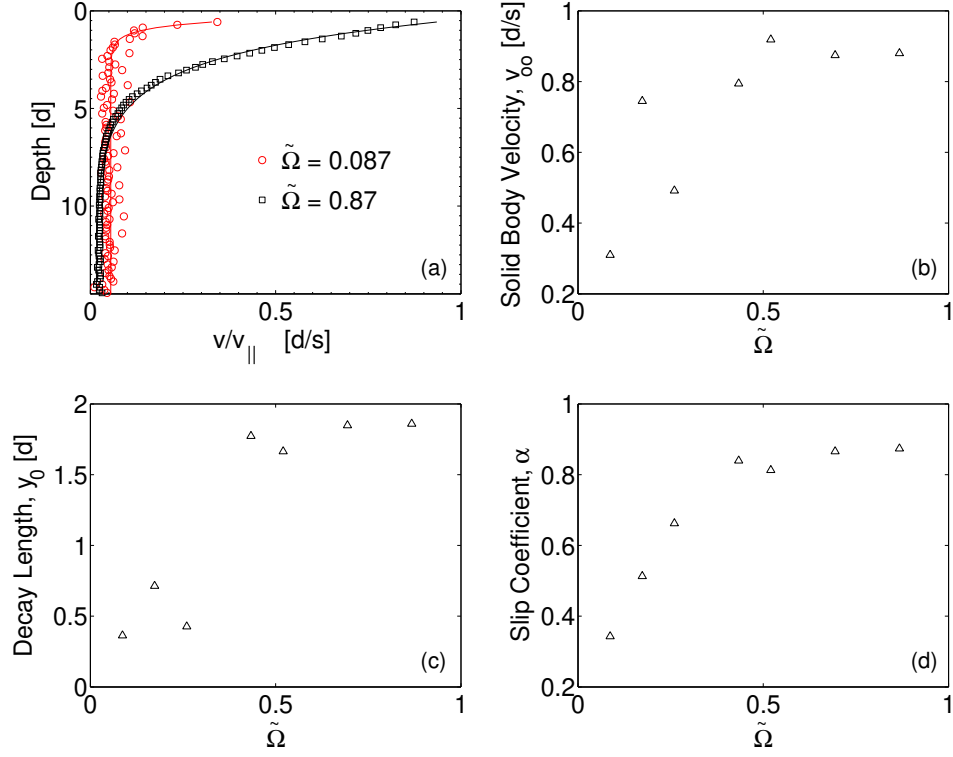


Figure 4. Characterization of velocity profiles at  $\Omega = 2.0$  and various  $\tilde{\Omega}$ . (a) Azimuthal velocity measured at outer wall as a function of depth measured. Lines are fits to Equation (3). (b) Solid body rotation  $v_1$  as a function of  $\tilde{\Omega}$ , (c) decay length  $y_0$  as a function of  $\tilde{\Omega}$  and (d) slip coefficient  $\alpha$  as a function of  $\tilde{\Omega}$ .

granular-gas like behavior. Further experiments varying  $(L; M; N)$  will be necessary to discover which of these determine the high- $\tilde{\Omega}$  boundary of the crystallized phase. In addition, the parameter  $H$  controls finite size effects.

#### 4. Shear Localization

Granular materials commonly exhibit shear banding, with an exponentially decaying velocity profile away from the shearing surface. As shown in Figure 4a, this shear band behavior is seen in both the crystallized ( $\tilde{\Omega} = 0.087$ ) and disordered states ( $\tilde{\Omega} = 0.87$ ) for  $\Omega = 2.0$ . To obtain the velocity profiles, we tracked individual particles visible at the outer wall using a high-speed video camera and determined trajectories for each. We then binned the resulting velocity components by depth to construct velocity profiles.

We characterize the azimuthal velocity,  $v(y)$ , by fitting the profile to the form

$$v(y) = v_1 + v_k e^{-y/y_0} \quad (3)$$

where  $v_1$  is the solid-body motion at the bottom plate,  $v_k$  is the known azimuthal velocity of the shear wheel at the outer wall,  $\alpha$  is the efficiency with which that velocity is transmitted to the top layer of granular material, and  $y_0$  is the decay length of the velocity with depth.

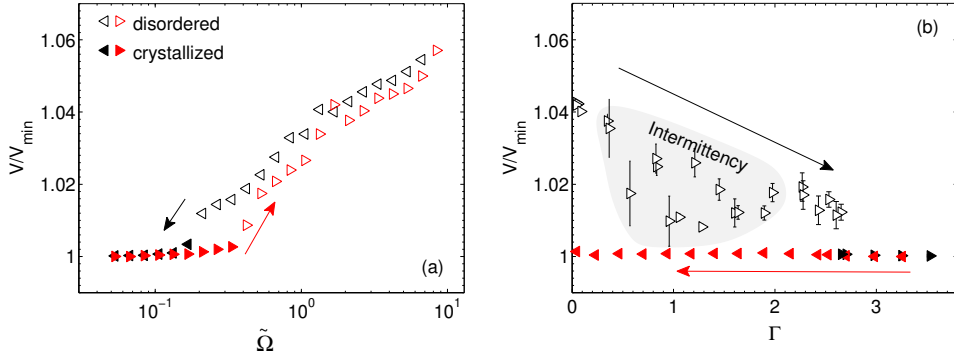


Figure 5. Volume  $V$  of cell, scaled by minimum observed volume  $V_{\min}$  as a function of (a)  $\tilde{\Omega}$  (at  $\tilde{\Omega} = 2.0$ ) and (b)  $\Gamma$  (at  $\tilde{\Omega} = 0.27$ ). Triangles point in direction of steps.

In the crystallized state, the shear is localized almost entirely to the first layer of particles (snally<sub>0</sub>), while in the disordered state the shear band extends several particles into the layer. The slip at the upper plate is lowest in the disordered state, where the uppermost particles are in constant contact with the shearing wheel. Note that the system is more dilated in the disordered state, and has a larger pressure [3]. While the disordered state has greater slip ( $v_1$ ) at the bottom plate, the scaled slip values ( $v_1 = v_k$ ) are in fact lower than in the crystallized state, visible in Figure 4a. For disordered states with  $\tilde{\Omega} < 0.4$ , the shear bands appear to have reached a steady state since they are all parameterized by the same values.

## 5. Transition

We examined the transition from the disordered to the crystallized state by first preparing a disordered state at high  $\tilde{\Omega}$ , then adjusting  $\tilde{\Omega}$  to the value of interest. We then performed two runs, one at constant  $\tilde{\Omega} = 0.27$  (starting from  $\tilde{\Omega} = 0$ ) and the other at constant  $\tilde{\Omega} = 2$  (starting from  $\tilde{\Omega} = 8.4$ ). The mean volume measured for each step of these two runs is shown in Figure 5.

For steps of decreasing  $\tilde{\Omega}$  (Figure 5a) the system compacts logarithmically until reaching  $\tilde{\Omega}_c$ , after which the system undergoes a first order phase transition to the crystallized state. Below  $\tilde{\Omega}_c$  only a small amount of additional compaction occurs, to a state with a volume  $V_{\min}$ , for which the packing fraction is  $\phi = 0.69$ . When  $\tilde{\Omega}$  is increased, the transition back to the disordered state is hysteretic, occurring for  $\tilde{\Omega}_h \approx 2 \tilde{\Omega}_c$ .

For steps of increasing  $\tilde{\Omega}$  (Figure 5b) the system also compacts. However, runs approaching the transition are difficult to repeat quantitatively, since there is a great deal of intermittency in the cell volume (see Figures 5b, 8a and [3] for details). For

$\tilde{\Omega} > \tilde{\Omega}_c$  the system is in the crystallized state. The transition also appears to be first order, but in this case the hysteresis is so extreme that the material was not observed to re-expand when we decreased  $\tilde{\Omega}$ .

We wish to understand why a crystallized state can disorder by increasing  $\tilde{\Omega}$ , but

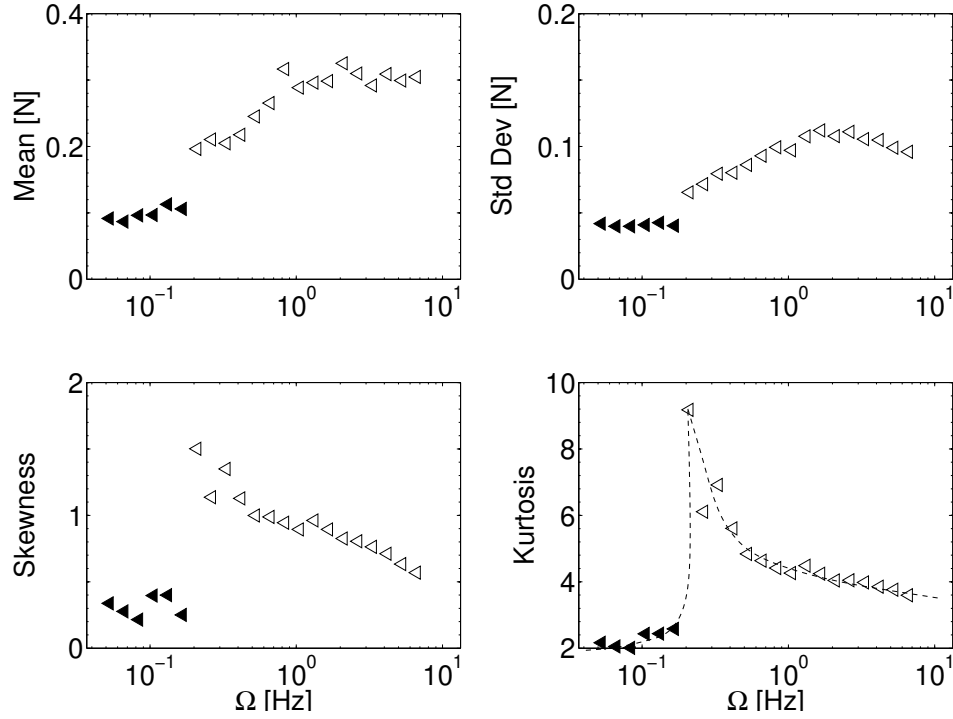


Figure 6. Characteristics of force probability distributions as a function of  $\Omega$  at  $\dot{\gamma} = 2:0$ . Triangles point in direction of steps in  $\dot{\gamma}$ ; solid points are crystallized phase; dashed line is guide to the eye.

not by decreasing  $\dot{\gamma}$ . In the case of increasing  $\dot{\gamma}$ , the stick-slip behavior in the top layers of the crystallized state is affected by the speed of the upper shearing wheel. As  $\dot{\gamma}$  increases, more horizontal momentum is transferred to the upper layer of balls, which results in longer regions of flowing particles. Eventually, the whole layer can be seen to mobilize and the disordering begins to take place throughout the cell. In contrast, for increases in  $A$  (and hence  $\dot{\gamma}$ ) no such increased momentum transfer takes place, and the results are similar to the irreversibility observed for compaction by tapping [4]. This transition shows some similarity to the "freezing-by-heating" transition seen in [13], in which individual particles with tunable noise are seen to crystallize as their noise level is increased. Such a system also shows hysteresis in returning to the disordered, mobilized state.

For the run at  $\dot{\gamma} = 2:0$ , seen in Figure 5a with steps downward in  $\dot{\gamma}$ , we observe signatures of the phase transition from disorder to crystallization via both the volume fluctuations and the force distribution, as shown in Figures 6 and 7. As  $\dot{\gamma} \rightarrow 0$  from above, both the volume fluctuations (measured from the variance of  $V(t)$ ) and the breadth of the force distribution (measured by the kurtosis, or fourth scaled moment, of  $F(t)$  on the force sensor) become large. In addition, the first order nature of the transition is visible in other characteristics of the force distribution, such as the mean, standard deviation, and skewness (see also Figure 3).

In granular systems, Edwards and coworkers [14] have introduced a temperature-like



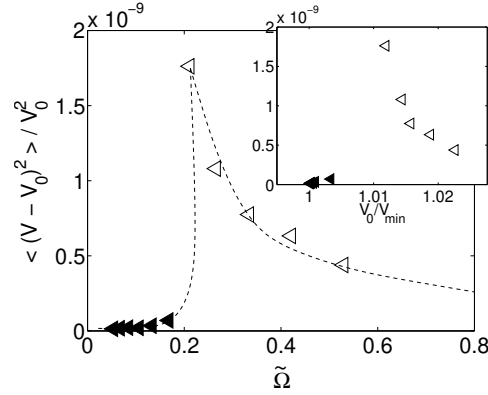


Figure 7. Volume fluctuations as a function of  $\tilde{\Omega}$ , scaled by average volume  $V_0$ . Inset: Volume fluctuations as a function of  $V_0 = V_{min}$  at each  $\tilde{\Omega}$ . Triangles point in direction of steps in  $\tilde{\Omega}$ ; solid points are crystallized phase; dashed line is guide to the eye.

measure, the compactivity, defined as  $X = (\partial V / \partial S)_N$  by analogy with thermodynamics. The central idea is that lower packing fractions correspond to a greater freedom for particle rearrangement, and hence a higher compactivity. In the statistical mechanics of ordinary second order phase transitions, susceptibilities such as  $(\partial^2 A / \partial T^2)_V$  (for free energy  $A$ ) are singular at the critical point. For example, the specific heat at constant volume is  $C_V = (\partial E / \partial T)_V = T (\partial^2 A / \partial T^2)_V$ . When described in terms of fluctuation-dissipation relations,  $k_B T^2 C_V = \hbar \langle (E - E_0)^2 \rangle$ , where  $E$  is the energy of the system and  $E_0$  its mean value. One expects energy fluctuations, and hence  $C_V$ , to be singular at the critical temperature  $T_c$ . By contrast, at a first order transition, discontinuities occur in densities, but one does not expect divergent fluctuations. Since  $V$  has taken the place of  $E$  in the Edwards formalism, the hallmark of a critical transition is increased fluctuations in the volume of the system as we approach  $X_c$ , the critical compactivity. In our experiments, volume (and hence  $X$ ) is set by  $\tilde{\Omega}$ , and the inset to Figure 7 shows apparently singular behavior for the volume fluctuations as a function of the volume. It is interesting that in these experiments, we see a discontinuity in the density, but also an indication of a singularity in the volume fluctuations. The magnitude of the fluctuations observed in the disordered state is similar to those observed in [15], where the standard deviation of the packing fraction is approximately  $10^{-4}$ .

## 6. Intermittency

The apparently singular volume fluctuations near  $J = 1$  come from the fact that the system exhibits intermittency in its state. The system is in fact spatially inhomogeneous, with instances of small  $V$  being crystallized in the majority of the cell and instances of large  $V$  being majority disordered. By examining the properties of the system in this intermittent regime, we are able to compare a broad range of states for nearly the same parameter values. The only varying parameters are the volume and pressure of the system, which are related to each other by a proportionality constant due to the

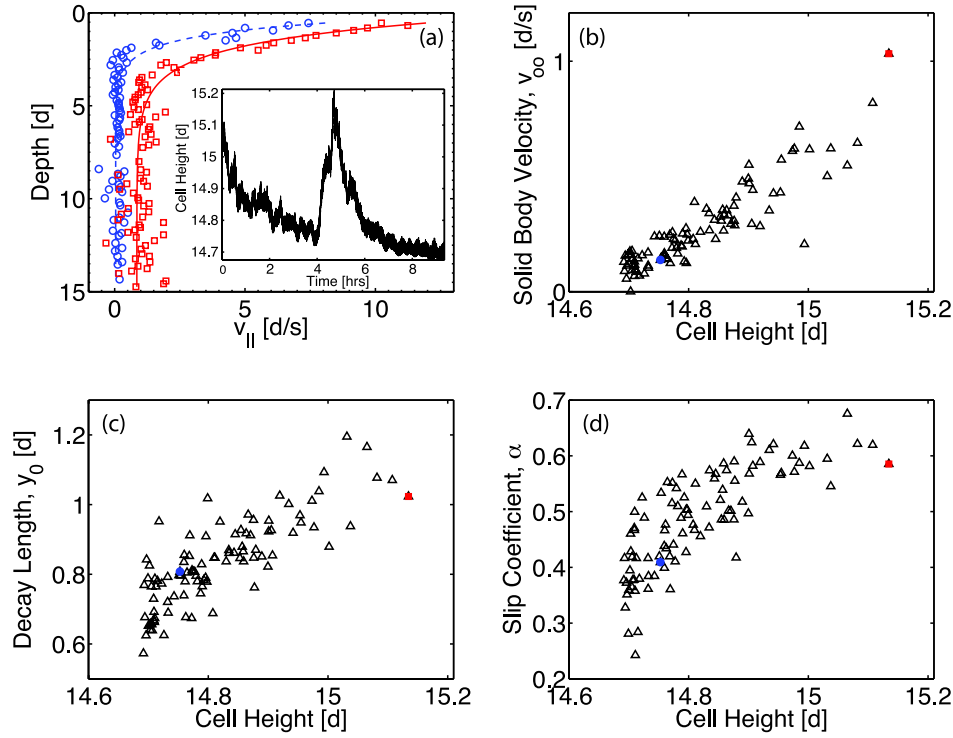


Figure 8. Characterization of velocity profiles in intermittent regime at  $\tilde{\omega} = 0.27$  and  $\Omega = 1.0$ . (a) Azimuthal velocity measured at outer wall as a function of depth measured for compact ( $\Omega = 1.0$ ,  $t = 3.8$  hrs) and dilated ( $\Omega = 1.0$ ,  $t = 4.7$  hrs) states. Lines are fits to Equation (3). (b) Solid body rotation  $v_0$  as a function of cell height, (c) decay length  $y_0$  as a function of cell height and (d) slip coefficient  $\alpha$  as a function of cell height. Solid symbols correspond to data from (a).

spring constant of the shaker [3].

The inset to Figure 8a shows a time series of the cell height for such a run, with  $\Omega = 1.0$  and  $\tilde{\omega} = 0.27$ . The system started from a dilated state and progressed to a majority crystallized state before re-dilating and re-compacting to an even more crystallized state over the course of approximately 10 hours. We again obtain velocity profiles at the outer wall, in this case while simultaneously monitoring the position of the bottom plate.

Figure 8a shows two velocity profiles from compact and dilated states. Because the system is spatially inhomogeneous, the particles in view of the camera may in fact be either disordered or crystallized at any given time during these measurements, regardless of the height of the cell. Importantly, the fit parameters in Figure 8b-d show the same trends as those in Figure 4 when rotation rate  $\tilde{\omega}$  is taken as a proxy for cell height. In both cases, we observe a continuum of states as the system moves between crystallization (compaction) and disorder (dilation). Again, it is interesting to note that the volume and pressure fluctuations are associated with the formation and melting of ordered clusters over time. Such behavior is characteristic of near-critical behavior. By contrast, at a thermodynamic first order transition, we would not expect to see persistent dominant

uctuations.

## 7. Discussion

The two characterizations of a transition in the system we discuss above provide contrasting, but complementary, information about the nature of the crystallizing phase transition in sheared and vibrated granular materials. The canonical hallmark of a transition to a jammed/glassy state is the continuous growth of the viscosity. Glass transitions do not in general contain first-order-like signatures, such as discontinuities in the volume or specific heat [16]. For sheared colloids, there are large stress fluctuations near a jamming transition [17], and in simulations of Lennard-Jones particles, force PDFs are observed to broaden [18, 19]. Similar behavior is observed in this system as well, but with a density discontinuity. By contrast, jammed/glassy states are all disordered, while the granular system described in this paper makes a transition to a crystallized state. In both the glassy and crystallized cases, however, the final states are unable to rearrange.

We observe similarities to critical phenomena in the increased volume fluctuations near the transition, a hallmark at odds with a glass transition. These fluctuations are similar to the density fluctuations observed at the liquid-gas critical point, which occur at diverging length scales. Therefore, further investigations into the nature of this transition should examine what length scales and order parameters are present, including a determination of the sizes of clusters and the spatial correlations between forces. Finally, we have introduced a number of dimensionless control parameters whose effects remain to be investigated in future studies.

## Acknowledgments

This research was supported by the NASA Microgravity program under grant NNC 04G B 08G, and North Carolina State University.

## References

- [1] H. M. Jaeger, S. R. Nagel, and R. P. Behringer. Granular solids, liquids, and gases. *Reviews Of Modern Physics*, 68:1259{1273, Oct 1996.
- [2] J. C. T. sai, G. A. Voth, and J. P. Gollub. Internal granular dynamics, shear-induced crystallization, and compaction steps. *Physical Review Letters*, 91:064301, Aug 8 2003.
- [3] K. E. Daniels and R. P. Behringer. Hysteresis and competition between disorder and crystallization in sheared and vibrated granular flow. *Physical Review Letters*, 94:168001, Apr 29 2005.
- [4] E. R. Nowak, J. B. Knight, M. L. Povinelli, H. M. Jaeger, and S. R. Nagel. Reversibility and irreversibility in the packing of vibrated granular material. *Powder Technology*, 94:79{83, Nov 1997.
- [5] A. Prevost, P. Melby, D. A. Egolf, and J. S. Urbach. Nonequilibrium two-phase coexistence in a confined granular layer. *Physical Review E*, 70:050301, Nov 2004.
- [6] S. B. Savage and M. Sayed. Stresses developed by dry cohesionless granular materials sheared in an annular shear cell. *Journal Of Fluid Mechanics*, 142:391{430, 1984.

- [7] B. M. J. Miller, C. O'Hern, and R. P. Behringer. Stress fluctuations for continuously sheared granular materials. *Physical Review Letters*, 77:3110{3113, Oct 7 1996.
- [8] W. Losert, L. Bocquet, T. C. Lubensky, and J. P. Gollub. Particle dynamics in sheared granular matter. *Physical Review Letters*, 85:1428{1431, Aug 14 2000.
- [9] D. M. Mueth, G. F. Debregeas, G. S. Karcmar, P. J. Eng, S. R. Nagel, and H. M. Jaeger. Signatures of granular microstructure in dense shear flows. *Nature*, 406:385{389, Jul 27 2000.
- [10] S. Nasuno, A. Kudrolli, and J. P. Gollub. Friction in granular layers: Hysteresis and precursors. *Physical Review Letters*, 79:949{952, Aug 4 1997.
- [11] J. C. Tsai and J. P. Gollub. Slowly sheared dense granular flows: Crystallization and nonunique final states. *Physical Review E*, 70:031303, Sep 2004.
- [12] G. D. R. M. Di. On dense granular flows. *European Physical Journal E*, 14, 2004.
- [13] D. Helbing, I. J. Farkas, and T. Vicsek. Freezing by heating in a driven mesoscopic system. *Physical Review Letters*, 84:1240{1243, Feb 7 2000.
- [14] S. F. Edwards and R. B. S. Oakeshott. Theory of powders. *Physica A*, 157:1080{1090, Jun 15 1989.
- [15] M. Schroter, D. I. Goldman, and H. L. Swinney. Stationary state volume fluctuations in a granular medium. *Physical Review E*, 71(3):030301, Mar 2005.
- [16] S. Torquato. Glass transition { hard knock for thermodynamics. *Nature*, 405:521{522, Jun 1 2000.
- [17] D. Lootens, H. van Damme, and P. Hebraud. Giant stress fluctuations at the jamming transition. *Physical Review Letters*, 90:178301, May 2 2003.
- [18] C. S. O'Hern, S. A. Langer, A. J. Liu, and S. R. Nagel. Force distributions near jamming and glass transitions. *Physical Review Letters*, 86:111{114, Jan 1 2001.
- [19] J. H. Snoeijer, T. J. H. Vlugt, M. van Hecke, and W. van Saarloos. Force network ensemble: A new approach to static granular matter. *Physical Review Letters*, 92:054302, Feb 6 2004.